

# Light-Scattering Study of Coil-to-Globule Transition of a Poly(*N*-isopropylacrylamide) Chain in Deuterated Water

Xiaohui Wang<sup>†</sup> and Chi Wu<sup>\*,†,‡</sup>

Department of Chemistry, The Chinese University of Hong Kong, Shatin, N. T., Hong Kong, and The Open Laboratory of Bond Selective Chemistry, Department of Chemical Physics, University of Science and Technology of China, Hefei, China

Received February 19, 1999; Revised Manuscript Received April 30, 1999

**ABSTRACT:** Using a nearly monodisperse ( $M_w/M_n < 1.1$ ) high molar mass ( $1.3 \times 10^7$  g/mol) poly(*N*-isopropylacrylamide) (PNIPAM), we studied the conformation change of individual PNIPAM chains between an extended random coil and a fully collapsed thermodynamically stable single chain globule in an extremely dilute D<sub>2</sub>O solution ( $\sim 6.3 \times 10^{-7}$  g/mL) by a combination of static and dynamic laser light scattering (LLS). In comparison with PNIPAM in H<sub>2</sub>O, the  $\Theta$ -temperature of PNIPAM in D<sub>2</sub>O is slightly higher, shifting from 30.6 to 32.1 °C. Moreover, the coil-to-globule transition in D<sub>2</sub>O showed no molten globular state, different from PNIPAM in H<sub>2</sub>O. However, the molten globular state exists in the globule-to-coil transition in D<sub>2</sub>O. The size of the PNIPAM chains near the  $\Theta$ -temperature in the globule-to-coil transition is smaller than that in the coil-to-globule transition; i.e., there exists a hysteresis, similar to PNIPAM in H<sub>2</sub>O. The hysteresis can be attributed to the intrachain interaction formed in the globular state. Our results indicate that the PNIPAM chains are stiffer in D<sub>2</sub>O than in H<sub>2</sub>O.

## Introduction

As a fundamental problem in polymer physics, the coil-to-globule transition has been extensively studied both in theories and in experiments over the past four decades.<sup>1–9</sup> Recently, using a nearly monodisperse high molar mass poly(*N*-isopropylacrylamide) (PNIPAM) sample, we successfully, for the first time, made the coil-to-globule-to-coil transition possible.<sup>9</sup> We also found that there exist two states, the crumpled coil and the molten globule, in the transition. In neutron scattering and nuclear magnetic resonance (NMR), to see how a long polymer chain can be packed into a small volume, deuterated water (D<sub>2</sub>O) has to be used to increase the contrast. Our previous study showed that deuterating a polystyrene chain could affect the chain flexibility around its  $\Theta$ -temperature.<sup>10</sup> Therefore, it is interesting to find whether the coil-to-globule-to-coil transition of PNIPAM in D<sub>2</sub>O is different from that in H<sub>2</sub>O.

## Experimental Section

**Sample Preparation.** The synthesis and fractionation of high molar mass PNIPAM samples were described before.<sup>7,9</sup> Deuterated water (D<sub>2</sub>O, 99.5% D, Aldrich) was used without further purification. We first prepared a stock solution ( $2.50 \times 10^{-5}$  g/mL). The solution was stood at room temperature for 1 week to ensure a complete dissolution. The stock solution was further diluted to a concentration in the range  $2.50 \times 10^{-5}$ – $5.07 \times 10^{-6}$  g/mL and filtered by using a 0.5  $\mu$ m Millipore Millex-LCR filter. A combination of fractionation and filtration finally led to an extremely dilute solution ( $6.3 \times 10^{-7}$  g/mL) containing narrowly distributed ( $M_w/M_n < 1.1$ , estimated from the relative line width,  $\mu_2/\Gamma^2$ , obtained in dynamic light scattering, i.e.,  $M_w/M_n \sim 1 + 4\mu_2/\Gamma^2$ ) high molar mass ( $1.3 \times 10^7$  g/mol) PNIPAM chains.

**Laser Light Scattering (LLS).** In static LLS, the angular dependence of the excess absolute time-average scattered intensity, known as the Rayleigh ratio  $R_{v}(q)$ , of a dilute

polymer solution at concentration  $C$  (g/mL) and the scattering angle  $\theta$  was measured.  $R_{v}(q)$  is related to the weight-average molar mass  $M_w$ , the root-mean-square radius of gyration ( $R_g^2$ )<sup>1/2</sup> (or written as  $\langle R_g \rangle$ ), and polymer concentration  $C$  as<sup>11</sup>

$$\frac{KC}{R_{v}(q)} \cong \frac{1}{M_w} \left( 1 + \frac{1}{3} \langle R_g^2 \rangle q^2 \right) + 2A_2 C \quad (1)$$

where  $K = 4\pi^2 n^2 (dn/dC)^2 / N_A \lambda_0^4$  and  $q = (4\pi n / \lambda_0) \sin(\theta/2)$  with  $N_A$ ,  $dn/dC$ ,  $n$ ,  $\lambda_0$ , and  $\theta$  being the Avogadro number, the specific refractive index increment, the solvent refractive index, the wavelength of light in vacuo, and the scattering angle, respectively.  $A_2$  is the second virial coefficient. For an extremely dilute solution, the angular dependence of  $R_{v}(q)$  directly leads to  $M_w$  and  $\langle R_g \rangle$ .

In dynamic LLS,<sup>12,13</sup> the cumulant analysis of the measured intensity–intensity time correlation function  $G^2(t)$  of narrowly dispersed polymer chains in a dilute solution is sufficient to determine an accurate average line width ( $\langle \Gamma \rangle$ ). For a diffusive relaxation,  $\langle \Gamma \rangle$  is related to the average translational diffusive coefficient by  $\langle D \rangle = \langle \Gamma \rangle / q^2$  and the average hydrodynamic radius by  $\langle R_h \rangle = k_B T / (6\pi\eta \langle D \rangle)$  with  $k_B$ ,  $\eta$ , and  $T$  being the Boltzmann constant, the solvent viscosity, and the absolute temperature, respectively. The Laplace inversion of  $G^2(t)$  by using the CONTIN program<sup>14</sup> leads to the hydrodynamic radius distribution  $f(R_h)$ .

The LLS instrumentation has been detailed before.<sup>7</sup> It should be noted that our LLS spectrometer has an unusual small angle range 6°–20°, very important for the study of the coil state of a long polymer chain because of the required condition of  $q \langle R_g \rangle \ll 1$ . The measured  $dn/dC$  of PNIPAM in D<sub>2</sub>O at  $T = 25$  °C and  $\lambda_0 = 532$  nm is  $0.232 \pm 0.001$  mL/g. The long-term temperature fluctuation inside the sample holder was less than  $\pm 0.02$  °C.

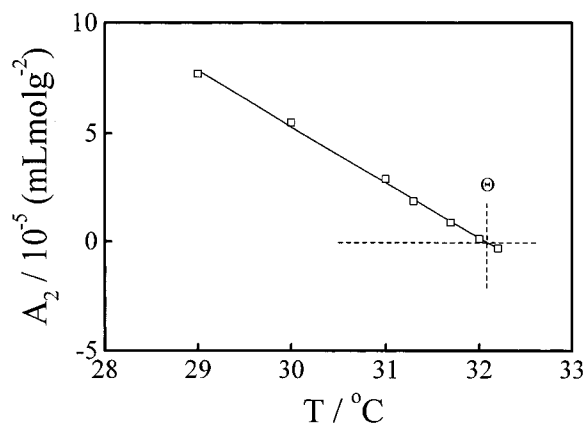
## Results and Discussion

Figure 1 shows that the second virial coefficient  $A_2$  decreases as the solution temperature increases, a characteristic of aqueous polymer solution because of the negative entropy change. The interpolation of  $A_2 \rightarrow 0$  led to the Flory  $\Theta$ -temperature (32.1 °C), which is higher than the  $\Theta$ -temperature (30.5 °C) of PNIPAM

<sup>†</sup> The Chinese University of Hong Kong.

<sup>‡</sup> University of Science and Technology of China.

\* To whom correspondence should be addressed.



**Figure 1.** Temperature dependence of the second virial coefficient  $A_2$  for PNIPAM in  $D_2O$ .

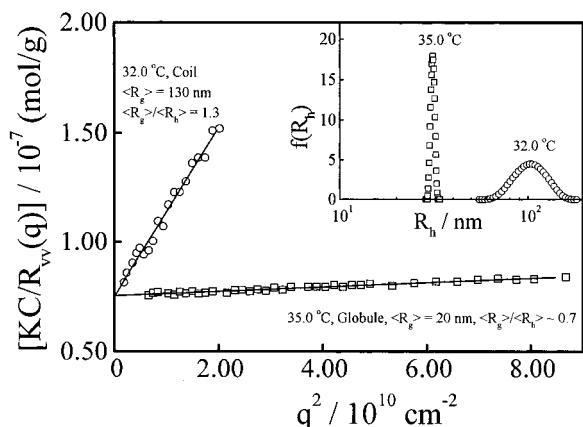
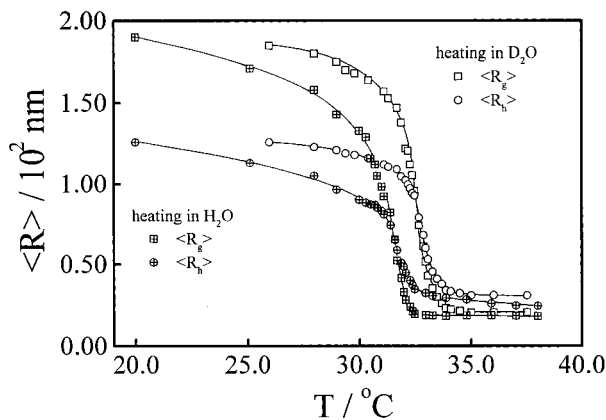


**Figure 2.** Typical angular dependence of  $KC/R_v(q)$  of the PNIPAM chains in  $D_2O$  at two different temperatures, where the polymer concentration is  $6.3 \times 10^{-7}$  g/mL. The inset shows the corresponding hydrodynamic radius distributions  $f(R_h)$  of the PNIPAM chains in the coil and the globule states.

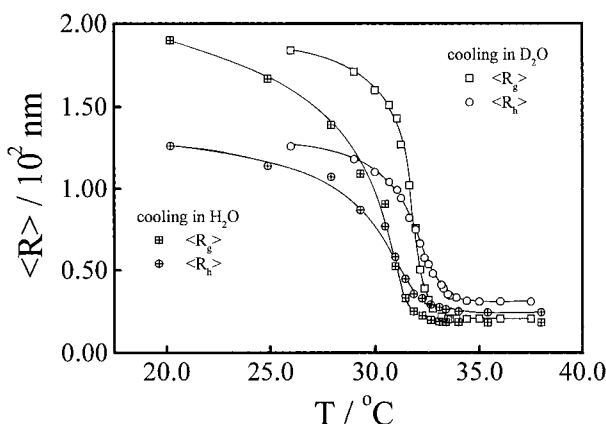
in  $H_2O$ , indicating that  $D_2O$  is a better solvent for PNIPAM than  $H_2O$ .

Figure 2 shows that after the temperature increases from 32 to 35 °C the slope of the line sharply decreases, reflecting a decrease of  $\langle R_g \rangle$  from 130 to 20 nm. It clearly indicates the collapse of the PNIPAM chains in  $D_2O$ . The chain collapse can be directly viewed from the change of hydrodynamic radius distribution  $f(R_h)$  as shown in the inset of Figure 1. The extrapolation of  $[KC/R_v(q)]_{q \rightarrow 0}$  led to the same intercept. On the basis of eq 1, this indicates no change in  $M_w$ ; i.e., the observed coil-to-globule transition was a pure intrachain process. It should be stated that the intensity of the scattered light ( $I$ ) in the globule state was independent of time, indicating that individual globules were stable because  $\langle I \rangle$  is proportional to  $M_w$  and  $M_w$  is further proportional to  $n_i M_i^2$  on the basis of eq 1, very sensitive to the interchain aggregation.

Figure 3 shows the temperature dependence of  $\langle R_g \rangle$  and  $\langle R_h \rangle$  of PNIPAM chains in the heating process, where each data point was obtained at least 2 h after the solution reached the desired temperature even though we knew that individual PNIPAM chains can reach the equilibrium state as fast as the temperature change.<sup>7</sup> Below 31.7 °C, the PNIPAM chains slightly shrinks as  $T$  increases, while in the temperature range 31.7–33.9 °C, both  $\langle R_g \rangle$  and  $\langle R_h \rangle$  dramatically decreases as  $T$  increases, indicating the coil-to-globule transition. Above 33.9 °C, both  $\langle R_g \rangle$  and  $\langle R_h \rangle$  were nearly independ-



**Figure 3.** Temperature dependence of the average radius of gyration ( $\langle R_g \rangle$ ) and hydrodynamic radius ( $\langle R_h \rangle$ ) of the PNIPAM chains in  $D_2O$  in the coil-to-globule (heating) transition. For comparison, the previous results of PNIPAM in  $H_2O$  were also plotted.



**Figure 4.** Temperature dependence of the average radius of gyration ( $\langle R_g \rangle$ ) and hydrodynamic radius ( $\langle R_h \rangle$ ) of the PNIPAM chains in  $D_2O$  in the globule-to-coil (cooling) transition. For comparison, the previous results of PNIPAM in  $H_2O$  were also plotted.

ent of the temperature, indicating that the PNIPAM chains reach the fully collapsed globular state. In comparison with our previous results of PNIPAM in  $H_2O$ , the average size of the PNIPAM chains in  $D_2O$  was larger. Therefore, the density of the globule in  $D_2O$  is slightly lower than that in  $H_2O$ .

Note that even at their respective  $\Theta$ -temperatures, the unperturbed PNIPAM chains in  $D_2O$  were more extended. It has been known that at  $\Theta$ -temperature the unperturbed chains have a size of  $\langle R \rangle = lN^{1/2}$ , where  $N$  is the number of segments per chain and  $l$  is the length of each segment. For a given PNIPAM chain, i.e., for a fixed contour length ( $lN$ ), larger  $\langle R \rangle$  means smaller  $N$  or larger  $l$ ; i.e., the chain are stiffer in  $D_2O$ . The fact that the same polymer chain under two different  $\Theta$ -temperatures has two different sizes can be attributed to different local conformations.

Figure 4 shows the temperature dependence of  $\langle R_g \rangle$  and  $\langle R_h \rangle$  of the PNIPAM chains in the cooling process. The profile is similar to that in the heating process, as shown in Figure 3. However, some points should be noted. (1)  $\langle R_g \rangle$  did not increase until  $T$  was cooled to 33.3 °C, while  $\langle R_h \rangle$  started to increase at 33.9 °C; (2) in the transition range 31.0–33.9 °C, the PNIPAM chains in the cooling process had a smaller size, revealing a hysteresis similar to the case of PNIPAM in  $H_2O$ , which

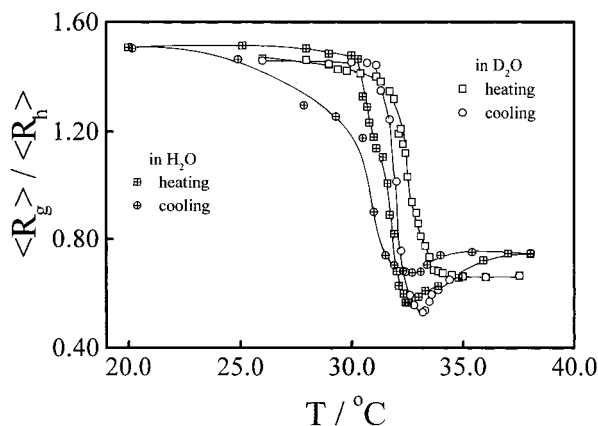


**Figure 5.** Temperature dependence of the ratio of the radius of gyration to the hydrodynamic radius ( $\langle R_g \rangle / \langle R_h \rangle$ ) of the PNIPAM chains in  $D_2O$  in the coil-to-globule (heating) and the globule-to-coil (cooling) transitions. For comparison, the previous results of PNIPAM in  $H_2O$  were also plotted.

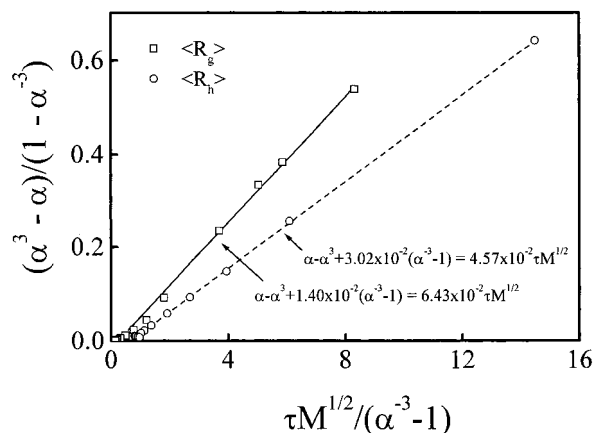
was attributed to the formation of some intrachain structures, presumably the intrachain hydrogen bonding, in the globular state.

Figure 5 shows that in both the heating and cooling processes  $\langle R_g \rangle / \langle R_h \rangle$  is nearly a constant ( $\sim 1.4$ ) when  $T$  is lower than the  $\Theta$ -temperature. In the transition range of the heating process,  $\langle R_g \rangle / \langle R_h \rangle$  decreases sharply from 1.4 to 0.7 and remains  $\sim 0.7$  when  $T > 33.7$  °C. In comparison with PNIPAM in  $H_2O$ ,  $\langle R_g \rangle / \langle R_h \rangle$  for PNIPAM in  $D_2O$  shows no dip, but in the cooling process,  $\langle R_g \rangle / \langle R_h \rangle$  has a dip around 33.1 °C, similar to the case of PNIPAM in  $H_2O$ . At the dip,  $\langle R_g \rangle / \langle R_h \rangle$  is only 0.54, corresponding to the molten globule state; i.e., the surface of the globule has a lower density than the center. A combination of Figures 4 and 5 shows that the dip of  $\langle R_g \rangle / \langle R_h \rangle$  is attributed to the increase of  $\langle R_h \rangle$  as the temperature decreases because  $\langle R_g \rangle$  is nearly a constant in the same temperature range. The missing of the dip in the heating process implies that the collapse of the PNIPAM chain in  $D_2O$  is more uniform from center to surface, which is different from that in  $H_2O$ .

Birshtein and Pryamitsyn suggested that the contraction factor  $\alpha$ , defined as  $\langle R \rangle_T / \langle R \rangle_\Theta$ , is related to the reduced temperature ( $\tau = (T - \Theta) / \Theta$ ) and the molar mass of a polymer chain ( $M$ ) by<sup>11</sup>

$$\alpha - \alpha^3 + C(\alpha^{-3} - 1) = B\tau M^{1/2} \quad (2)$$

where  $B$  and  $C$  are two constants, independent of  $M$  and  $T$  for a given polymer/solvent system. On the basis of eq 2, the plot of  $(\alpha^3 - \alpha) / (1 - \alpha^{-3})$  vs  $\tau M^{1/2} / (\alpha^{-3} - 1)$  is a straight line and give out the  $B$  and  $C$  as shown in Figure 6. The balance between the deformation of a Gaussian chain and the ternary-segment intrachain interaction, i.e.,  $\alpha - \alpha^3 = C(\alpha^{-3} - 1)$ , is defined as the crossover point from the coil region to the globule region. Our results show that the crossover points are far away



**Figure 6.** Plot of  $(\alpha^3 - \alpha) / (1 - \alpha^{-3})$  vs  $\tau M^{1/2} / (\alpha^{-3} - 1)$ , where  $\alpha = \langle R_g \rangle_T / \langle R_g \rangle_\Theta$  or  $\langle R_h \rangle_T / \langle R_h \rangle_\Theta$ . The solid and dashed lines respectively represent the best fitting of  $\alpha - \alpha^3 + C(\alpha^{-3} - 1) = B\tau M^{1/2}$ .

from the  $\Theta$ -temperature but close to the temperature at which  $\langle R_g \rangle$  and  $\langle R_h \rangle$  approach their respective constants. In comparison with PNIPAM in  $H_2O$ ,<sup>9</sup>  $C$  is nearly the same, which is expected because the ternary-segment intrachain interaction is independent of solvent, but  $B$  is larger, indicating a larger binary-segment interaction.

**Acknowledgment.** The financial support of the National 973 project (RE-05-02), the Research Grants Council of Hong Kong Special Administration Region Government Earmarked Grant 1998/99 (CUHK 4123, 2160111), and the National Distinguished Young Investigator Grant (1996, 29625410) is gratefully acknowledged.

## References and Notes

- (1) Sun, S. T.; Nishio, I.; Swislow, G.; Tanaka, T. *J. Chem. Phys.* **1980**, *73*, 5971.
- (2) Chu, B.; Park, I. H.; Wang, Q. W.; Wu, C. *Macromolecules* **1987**, *20*, 1965.
- (3) Kubota, K.; Fujishige, S.; Ando, I. *Polym. J.* **1990**, *22*, 15.
- (4) Birshstein, T. M.; Pryamitsyn, V. A. *Macromolecules* **1991**, *24*, 1554.
- (5) Meewes, M.; Ricka, J.; de Silva, M.; Nyffenegger, R.; Binkert, T. *Macromolecules* **1991**, *24*, 5811.
- (6) Grosberg, A. Y.; Kuznetsov, D. V. *Macromolecules* **1993**, *26*, 4249 and references therein.
- (7) Wu, C.; Zhou, S. *Macromolecules* **1995**, *28*, 8381 and references therein.
- (8) Ito, D.; Kubota, K. *Macromolecules* **1997**, *30*, 7828.
- (9) Wang, X.; Qiu, X.; Wu, C. *Macromolecules* **1998**, *31*, 2972.
- (10) Wang, X.; Xu, Z.; Wan, Y.; Huang, T.; Pispas, S.; Mays, J. W.; Wu, C. *Macromolecules* **1997**, *30*, 7202.
- (11) Zimm, B. H. *J. Chem. Phys.* **1948**, *16*, 1099.
- (12) Pecora, R. *Dynamic Light Scattering*; Plenum Press: New York, 1976.
- (13) Chu, B. *Laser Light Scattering*, 2nd ed.; Academic Press: New York, 1991.
- (14) Provencher, S. W. *Makromol. Chem.* **1979**, *180*, 201.

MA9902450